

545053



Sandia National Laboratories

Operated for the U.S. Department of Energy by
Sandia Corporation

LOCKHEED MARTIN

4100 National Parks Highway
Carlsbad, NM 88220
Phone: (505) 234-0001
Fax: (505) 234-0061
Email: bypark@sandia.gov

Date: December 21, 2006

To: Moo Y. Lee (6711)

From: Byoung Y. Park (6711)

John F. Holland (1524)

Technical Review: Courtney G. Herrick (6711)

QA Review: Mario J. Chavez (6710)

Management Review: Moo Y. Lee (6711)

Subject: Error in DRZ calculation in the Clay Seam G analysis

An error has been discovered in the ALGEBBRA script file used to calculate the disturbed rock zone (DRZ) around the disposal room and the shear failure zone (SFZ) in the anhydrite layers in "Structural Evaluation of WIPP Disposal Room Raised to Clay Seam G" [Park and Holland, 2004]. The purpose and methodology of the analysis are described in Park [2002]. The original results of the DRZ analyses were presented at the 40th U.S. Symposium on Rock Mechanics [Park et al., 2005].

During simulation for Bayou Choctaw strategic petroleum reserve (SPR) [Park et al., in preparation, 2006], we discovered a potentially significant error in the DRZ and SFZ calculation. This memorandum describes the error, scopes its potential importance, and provides recommendation for remediation.

Background

The US SPR stores crude oil in caverns located at salt domes in Texas and Louisiana. Most of the caverns were solution mined and are typified as cylindrical in shape. Geotechnical concerns arise due to the close proximity of the some of the caverns to each other or to the edge of salt. Potential damage to or around the SPR caverns was evaluated based on two criteria: dilatant damage and tensile failure. A dilatant damage criterion is used to delineate potential zones of damage in the salt formation surrounding SPR facilities. The dilatancy criterion used in SPR simulations is the same as that used in Clay Seam G analysis [Park and Holland, 2004] except the multiplication constant used is 0.257 rather than 0.27. To calculate the dilatancy damage potential in salt, the post-processing

PA 11/21/07 RM 1 of 18
WIPP:1.4.1.2:PLB:QA-L:PKG#531531

Information Only

code ALGEBRA is used to determine spatial locations of dilatant damage. During establishing the ALGEBRA scripts for SPR simulation, we found the scripts for Clay Seam G have an error.

Description of the Error

The following dilatancy criterion is used for calculation of the extent of the DRZ in the Clay Seam G analysis.

$$D = \frac{\sqrt{J_2}}{0.27I_1} \quad (1)$$

where D = damage factor

$I_1 = \sigma_1 + \sigma_2 + \sigma_3 = 3\sigma_m$: the first invariant of the stress tensor.

$\sqrt{J_2} = \sqrt{\frac{(\sigma_1 - \sigma_2)^2 + (\sigma_2 - \sigma_3)^2 + (\sigma_3 - \sigma_1)^2}{6}}$: the square root of the second invariant of the deviatoric stress tensor

$\sigma_1, \sigma_2,$ and σ_3 are the maximum, intermediate, and minimum principal stresses, respectively, and

σ_m is the mean stress.

When $D > 1$, the shear stresses in the salt (J_2) are large compared to the mean stress (I_1) and dilatant behavior is expected. When $D \leq 1$, the shear stresses are equal to or small compared to the mean stress and dilatancy is not expected.

The von Mises yield criterion is given by the following equation in terms of principal stresses,

$$\sigma_0 = \sqrt{\frac{(\sigma_1 - \sigma_2)^2 + (\sigma_2 - \sigma_3)^2 + (\sigma_3 - \sigma_1)^2}{2}} \quad (2)$$

where σ_0 is the so-called 'von Mises stress.'

$\sqrt{J_2}$ can be written in terms of von Mises stress as

$$\sqrt{J_2} = \frac{\sigma_0}{\sqrt{3}} \quad (3)$$

If the dilatancy potential (DPOT) is defined by

$$DPOT = \frac{\sqrt{J_2}}{I_1} = \frac{\sqrt{J_2}}{3\sigma_m} \quad (4)$$

DPOT can be rewritten in terms of von Mises stress and the mean stress as,

$$DPOT = \frac{\sigma_0/\sqrt{3}}{3\sigma_m} \quad (5)$$

In the original ALGEBRA script of Appendix B of the Clay Seam G report [Park and Holland, 2004] the factor $\sqrt{3}$ was not used to divide the von Mises stress in the numerator of Eq. 5. To incorporate this correction, the appropriate section of the original ALGEBRA file:

```

$
$ Compute mean pressure and limit it to 1.e-06
$
PRES = -( SIGXX + SIGYY + SIGZZ )/3.0
PRE = ABS(PRES) - 1.E-6
PRE2 = IFGZ(PRE,PRE,1.0E-6)
$
$ compute damage potential in the halite
$
BLOCKS 1 3
DPOT = VONMISES/(3.*ABS(PRE2))  ←
MDPOT = ENVMAX(DPOT)

```

should be changed to:

```

$
$ Compute mean pressure and limit it to 1.e-06
$
PRES = -( SIGXX + SIGYY + SIGZZ )/3.0
PRE = ABS(PRES) - 1.E-6
PRE2 = IFGZ(PRE,PRE,1.0E-6)
$
$ compute damage potential in the halite
$
BLOCKS 1 3
DPOT = (VONMISES/sqrt(3.0))/(3.*ABS(PRE2))  ←
MDPOT = ENVMAX(DPOT)

```

The anhydrite layer beneath the disposal room is expected to experience inelastic material behavior. The anhydrite layer marker bed is assumed to be isotropic and elastic until failure occurs. Failure is assumed to be governed by the Drucker-Prager (D-P) criterion:

$$\sqrt{J_2} = C - aI_1 \quad (6)$$

The Drucker-Prager constants, C and a are 1.35 MPa and 0.45, respectively. The values of C and a obtained by fitting both the yield and ultimate stress data for anhydrite [Morgan and Krieg, 1984]

When the safety factor, SF , is defined by

$$SF = \frac{C - aI_1}{\sqrt{J_2}} \quad (7)$$

SF can be rewritten in terms of von Mises stress and the mean stress as:

$$SF = \frac{1.35 + 0.45 \cdot 3.0 \cdot \sigma_m}{\sigma_o / \sqrt{3}} \quad (8)$$

Again, in the original ALGEBRA script of Appendix B of the Clay Seam G report [Park and Holland, 2004] the factor $\sqrt{3}$ was not used to divide the von Mises stress in the denominator of Eq. 8. To incorporate this correction, the appropriate section of the original ALGEBRA file:

```

$
$ compute drucker prager failure in the anhydrite
$
BLOCKS 2
PRE3 = IFEZ(PRE,1.0E-6,PRE)
SF1 = 0.45*PRE3*3. + 1.35
$
$ assume no tensile strength in the anhydrite
$
SF2 = IFGZ(SMAX,0.,SF1)
SF3 = IFLZ(SF2,0.,SF2)
$
SF = ABS(SF3)/VONMISES
MSF = ENVMIN(SF)

```

should be changed to:

```

$
$ compute drucker prager failure in the anhydrite
$
BLOCKS 2
PRE3 = IFEZ(PRE,1.0E-6,PRE)
SF1 = 0.45*PRE3*3. + 1.35
$
$ assume no tensile strength in the anhydrite
$
SF2 = IFGZ(SMAX,0.,SF1)
SF3 = IFLZ(SF2,0.,SF2)
$
SF = ABS(SF3)/(VONMISES/sqrt(3.0))
MSF = ENVMIN(SF)

```

Importance of the Error

This error is **not** significant to performance assessment (PA). The results of changes to the characteristics of the DRZ and shear failure of the anhydrite layers were not used in either PA for the original compliance certification application (CCA) [DOE, 1996] or the first compliance recertification application (CRA) [DOE, 2004].

Figure 1 shows an example comparison of the DRZ using the original ALGEBRA script with that using the corrected script at approximately 1 year for the gas generation factor $f=0.0$. Figure 2 shows an example comparison of the SFZ using the original ALGEBRA script with that using the corrected script at approximately 1 year for the gas generation factor $f=0.0$. MSF in the figure is the minimum value of SF over all previous time steps. It is defined in this manner because, unlike salt, once the anhydrite fails, it does not heal.

The size of DRZ using the original scripts is much larger than that using the corrected scripts. The size of SFZ using the original scripts is also larger than that using the corrected scripts. This error affects the sizes of both the DRZ and SFZ, thus it should be corrected, because DRZ size changes with time will be accounted for in BRAGFLO calculations in PA for next CRA in 2009.

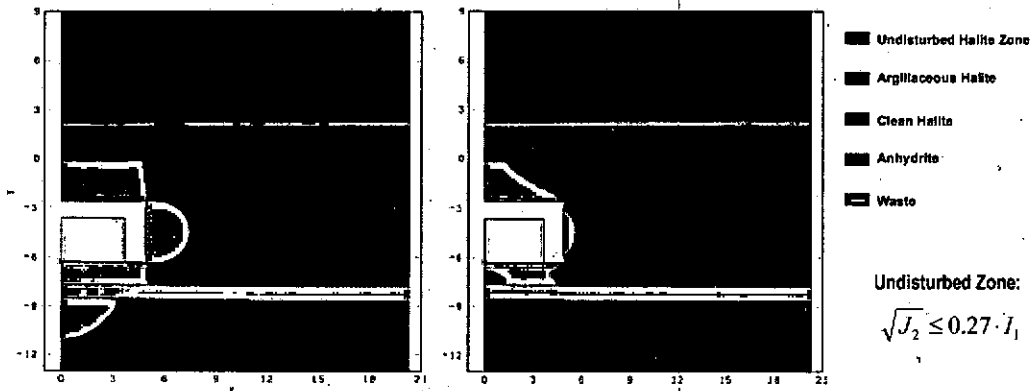


Figure 1: Comparison of the DRZ using the original ALGEBRA script (left) with that using the corrected script (right) at approximately 1 year for the gas generation factor $f=0.0$

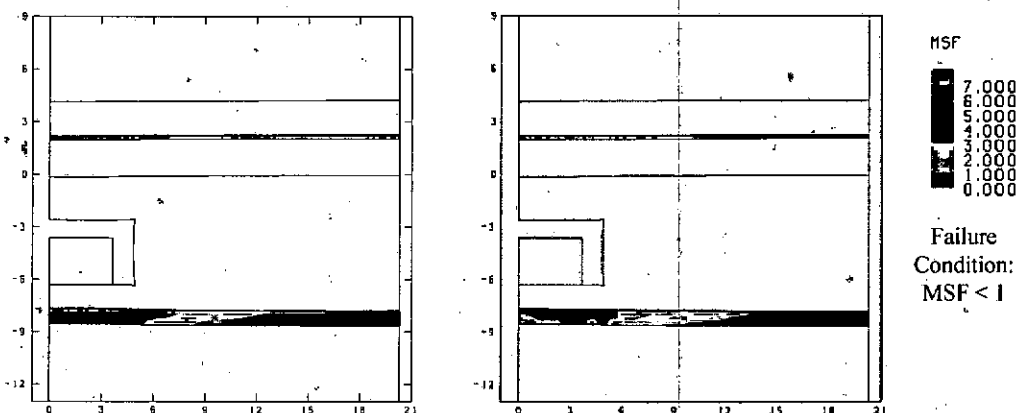


Figure 2: Comparison of the SFZ using the original ALGEBRA script (left) with that using the corrected script (right) at approximately 1 year for the gas generation factor $f=0.0$

Recommended Actions

The recommended course of action is to correct the error, to repeat the post-process, and to rewrite Section 7.4, 7.5, 8, and Appendix B in the report for Clay Seam G [Park and Holland, 2004]. The sections and appendix revised by the post-process using the corrected ALGEBRA scripts are provided in Appendix A of this memo. The files related to the correction will be stored in the subdirectory of /data/bypark/clayg/correction/ in the CVS.

References

DOE (U.S. Department of Energy), 1996. *Title 40 CFR Part 191: Compliance Certification Application for the Waste Isolation Pilot Plant*. DOE/CAO-1996-2184. U.S. Department of Energy, Carlsbad Area Office, Carlsbad, NM.

- DOE (U.S. Department of Energy), 2004. *Title 40 CFR Part 191 Subparts B and C: Compliance Recertification Application for the Waste Isolation Pilot Plant*. DOE/WIPP 2004-3231. U.S. Department of Energy, Carlsbad Field Office, Carlsbad, NM.
- Morgan, H.S. and R.D. Krieg, 1984, *Updated Drucker-Prager Constants for Anhydrite and Polyhalite*, Memorandum to D.E. Munson, dated June 19, 1984. Sandia National Laboratories, Albuquerque, New Mexico.
- Park, B.Y., 2002, *Analysis Plan for the Structural Evaluation of WIPP Disposal Room raised to Clay Seam G*, AP-093, Revision 1, Sandia National Laboratories, Carlsbad, NM (Copy on file in the Sandia WIPP Records Center as ERMS# 524805).
- Park, B.Y., B.L. Ehgartner, and M.Y. Lee, in preparation, *Three Dimensional Simulation for Bayou Choctaw Strategic Petroleum Reserve (SPR)*, SAND2006-draft, Sandia National Laboratories, Albuquerque, NM.
- Park, B.Y., F.D. Hansen, and M.Y. Lee, 2005, *Numerical Simulation of the Disturbed Rock Zone around Underground Openings in Rock Salt*, ARMA/USRMS 05-805, The 40th U.S. Symposium on Rock Mechanics (USRMS): Rock Mechanics for Energy, Mineral and Infrastructure Development in the Northern Regions, held in Anchorage, Alaska, June 25-29, 2005.
- Park, B.Y. and J.F. Holland, 2004, *Analysis Report for Structural Evaluation of WIPP Disposal Room Raised to Clay Seam G*. SAND2003-3409. Albuquerque, NM: Sandia National Laboratories.

Appendix A: Revision of Sections 7.4, 7.5, and Appendix B

Revision of Section 7.4 DRZ

Excavation of the repository and the consequent release of lithostatic stress create a disturbed rock zone (DRZ) around the underground openings. Fractures and microfractures within the DRZ increase porosity and permeability of the rock and could provide avenues for brine flow from the DRZ to the excavated opening. Salt creep is expected to close the fractures in the halite in the DRZ over time, exhibiting what is called the healing effect. In this section, the change of DRZ with time is provided through the interpretation of the SANTOS analyses results.

Figures 29 to 32 show the change with time of the DRZ around a disposal room raised 2.43 m above the current level for the gas generation factor $f=0.0, 0.4, 1.0$ and 2.0 . The undisturbed zone (dark blue zone) in the figures is defined by $D < 1$ in Equation 18 in Section 4. The most extensive DRZ occurs at early time, say in the first ten years after the opening is mined. As the back stress — caused by resistance to deformation of the waste stack — increases, the DRZ disappears according to the stress invariant criterion. The undisturbed zone no longer appears after the last time frame (6th frame) in the figures. This finding is consistent with other similar numerical simulations, such as Van Sambeek et al. (1993). They reported “A similar calculation for a brine-filled borehole or internally pressurized cavern shows that the thickness of the dilatancy zone depends on the internal pressure. The dilatancy zone around a cavern can be completely suppressed by an internal pressure equal to a small fraction of the lithostatic stress for the depth of the cavern.” Thus, calculations show that the damaged zone within the salt would heal.

The maximum extent of the DRZ calculated for the raised repository reaches approximately 3.8 m, the distance to the anhydrite layer (MB 139), below the room. The DRZ does not extend through the anhydrite layer that behaves as a buffer. The DRZ above the room disappears within a short period after the ceiling of room contacts the waste.

Modeling of the raised repository can be compared to Figures 33 to 36, which show the change of the DRZ around a disposal room at the current horizon with time for $f=0.0, 0.4, 1.0$ and 2.0 . The largest DRZ occurs early after the excavation for all f values, which is very similar to the case for the raised repository. The DRZ under the room does not extend through the anhydrite layer, in a manner similar to what happens in the case of the raised room. A maximum thickness of the DRZ is approximately 3.6 m over the roof of the room. The thickness of the DRZ in the floor of the present room is 1.4 m, the distance to the anhydrite layer. The DRZ does not extend through MB 139, the same as the case of the raised rooms.

In these calculations, gas production from corrosion and microbial activity initiates instantaneously. Internal gas pressure is a key concern when considering the DRZ evolution and devolution in terms of the modeling output. As noted previously, rooms in which no gas or minimal gas is produced will close completely around the waste, as shown in Figures 29 and 33. Gas production from inside the room affects room closure and characteristics of the DRZ. The stress conditions thus created in the rock salt would appear favorable for healing to occur, but it may be that healing would not occur because gas has entered the void space. If the inward creeping rock salt does not experience a solid, mechanical back stress, it will not heal. These concepts need to be taken into account when examining the DRZ figures, in which the DRZ is delineated based on the invariant stress criterion.

The vertical closure would evidently be sufficient to create a back stress in the vertical direction for all gas generation factors considered. The upper and lower salt DRZ would thereby be situated in a

stress field favorable for healing. The rib deformation, based on these models, is not sufficient to compress the waste laterally when gas is produced within the room.

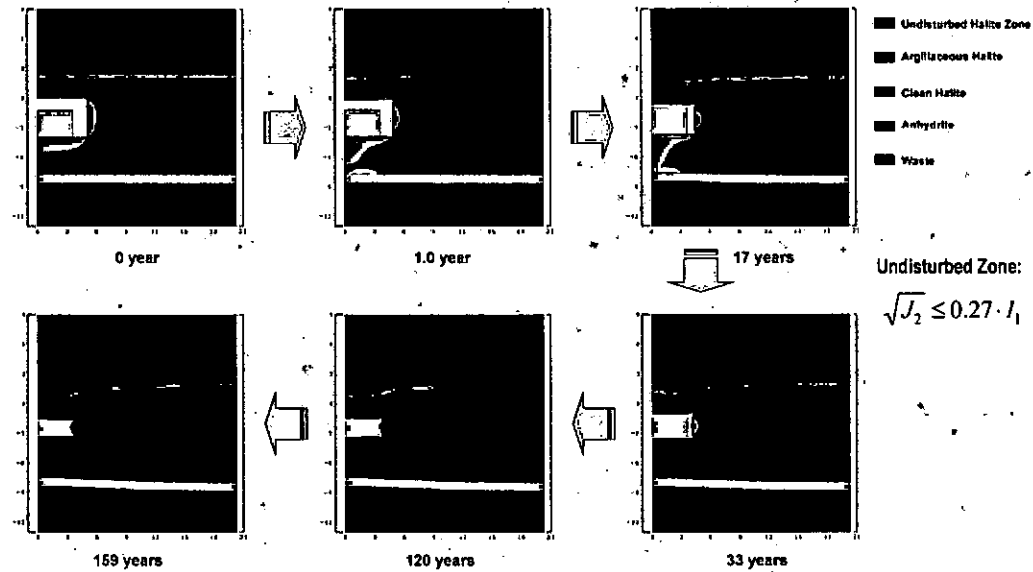


Figure 29: Change of the DRZ around a disposal room raised 2.43 m above the current level for the gas generation factor $f=0.0$

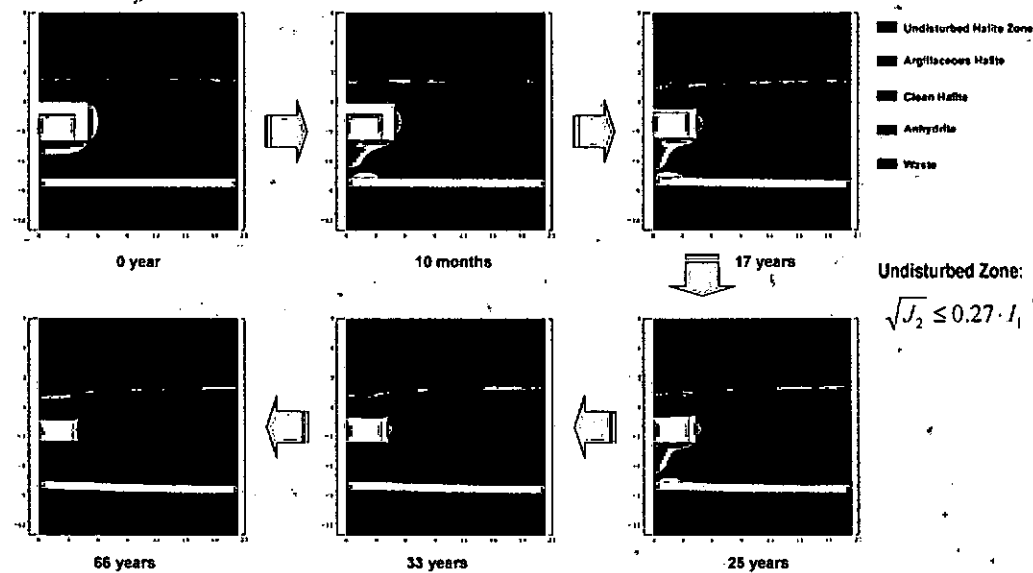


Figure 30: Change of the DRZ around a disposal room raised 2.43 m above the current level for the gas generation factor $f=0.4$

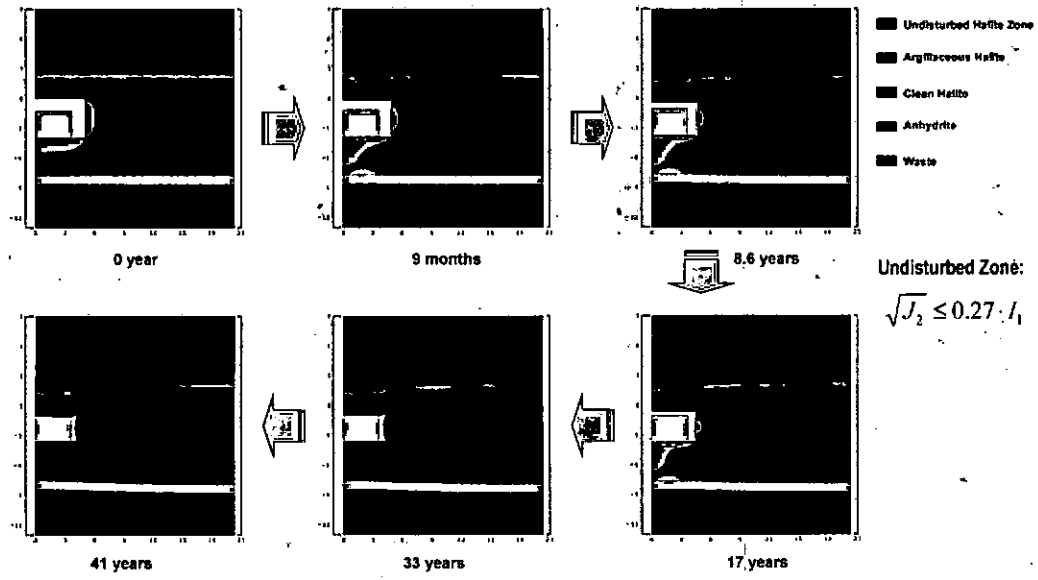


Figure 31: Change of the DRZ around a disposal room raised 2.43 m above the current level for the gas generation factor $f=1.0$

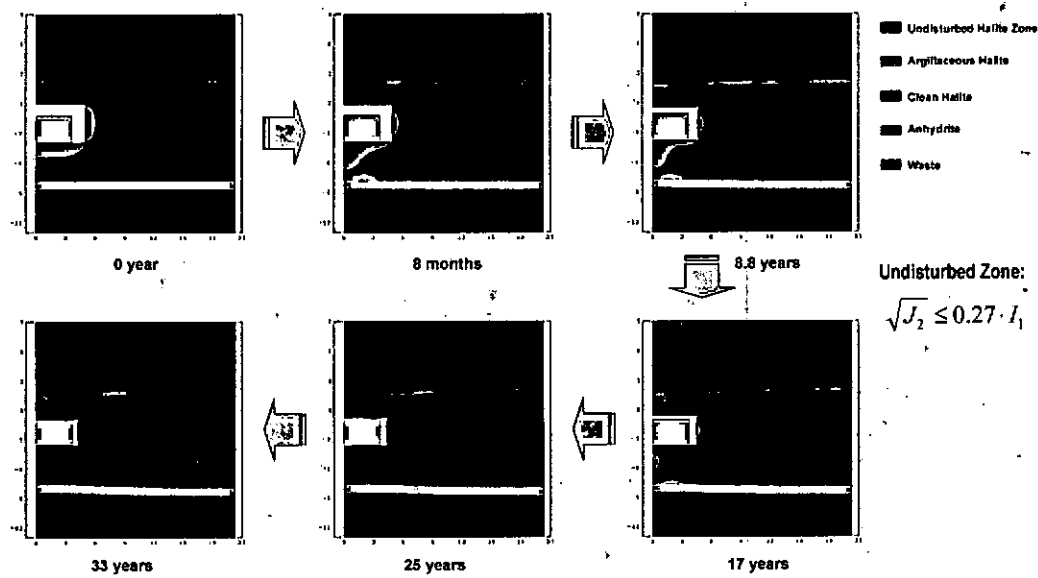


Figure 32: Change of the DRZ around a disposal room raised 2.43 m above the current level for the gas generation factor $f=2.0$

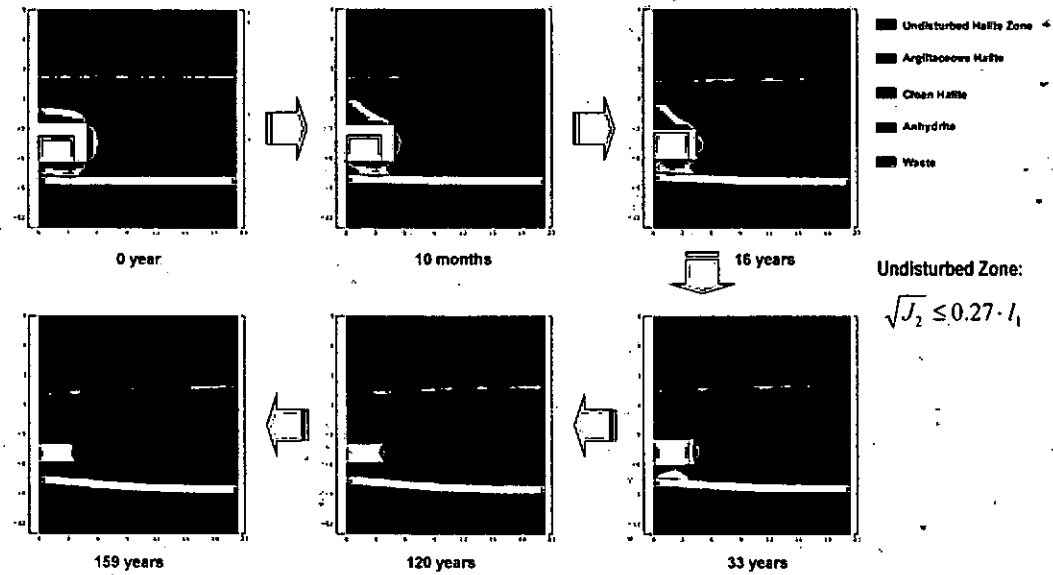


Figure 33: Change of the DRZ around a current disposal room for the gas generation factor $f=0.0$

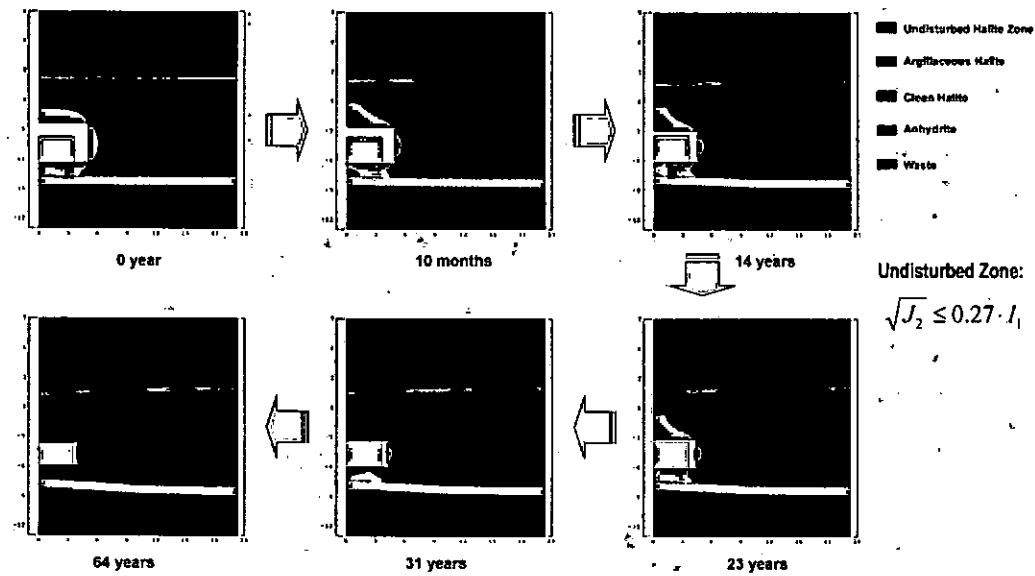


Figure 34: Change of the DRZ around a current disposal room for the gas generation factor $f=0.4$

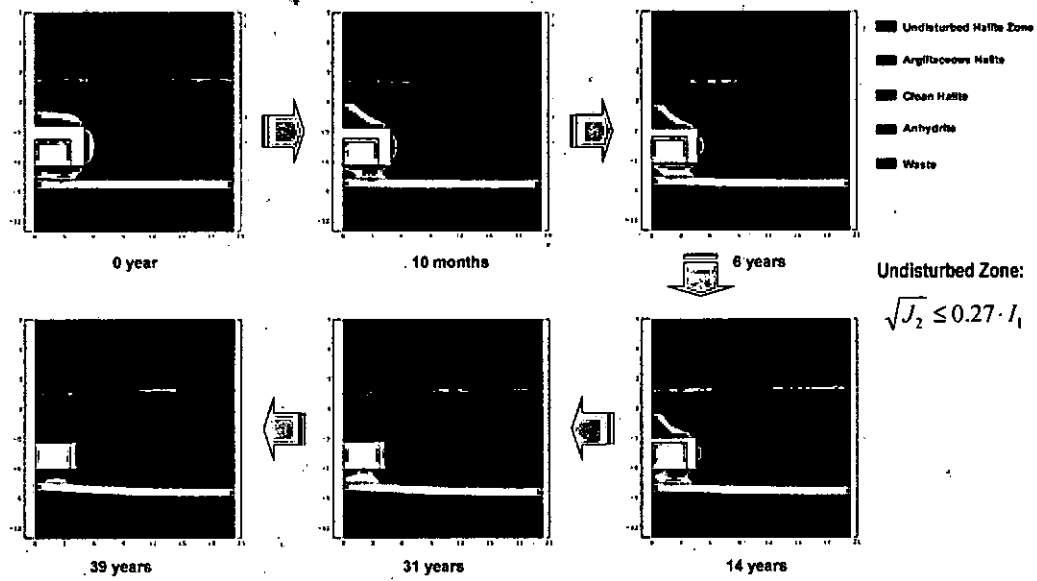


Figure 35: Change of the DRZ around a current disposal room for the gas generation factor $f=1.0$

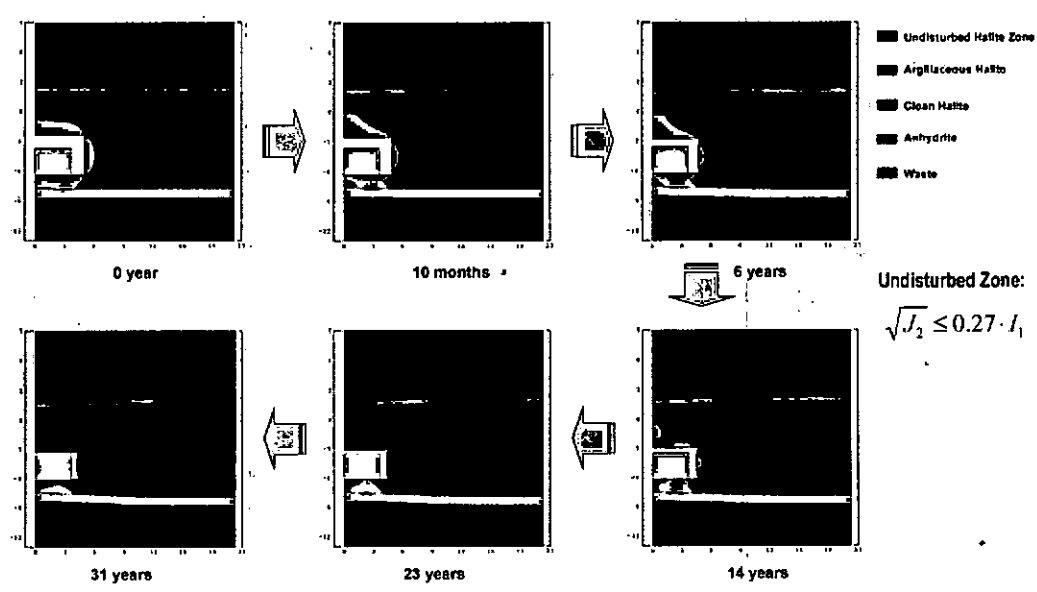


Figure 36: Change of the DRZ around a current disposal room for the gas generation factor $f=2.0$

Revision of Section 7.5 Shear Failures in Anhydrite

In this section, as discussed in Section 2.2.4, the shear failure pattern with time in the anhydrite is interpreted from the SANTOS output using the Drucker-Prager criterion. In the case of anhydrite, it is assumed that if $MSF < 1$, the shear failure will have occurred, and the tensile strength is zero. The MSF is the cumulative shear failure variable which is defined from Equation (12):

$$SF = \frac{C - aJ_1}{\sqrt{J_2}} \quad (19)$$

$$MSF = \text{Min} (SF) \quad (20)$$

MSF is the minimum value of SF over all previous time steps. It is defined in this manner because, unlike salt, once the anhydrite fails, it does not heal.

Figures 37 to 40 show the shear failure zones with time in the upper and the lower anhydrite layers of the disposal room being raised 2.43 m. The shear failure does not occur in either the upper or lower anhydrite layers at the moment of excavation, but appears above and below the middle of the pillar one day after the excavation. The shear stress in the anhydrite increases with time, therefore the extent of the failure zone also increases. The maximum extent of the shear failure zone occurs within the first 100 years. The internal gas pressure of the room does not affect the size of the failure zone in the anhydrite.

Figures 41 to 44 show the shear failure zone with time in the upper and the lower anhydrite layers of the present disposal room. The failure pattern of the present room is similar to the one of the raised room except the shear stress in the anhydrite for the present room increases faster than the raised room.

The distance between the bottom of the disposal room and the lower anhydrite layer is increased from 1.38 m to 3.81 m due to raising the room by 2.43 m. In other words, the current room is closer to Marker Bed 139. Because of this, the deformation of the anhydrite layer with the room closure is larger for the current room than the raised room. The shear failure zone is accordingly larger for the current room as shown in Figure 37 to 44.

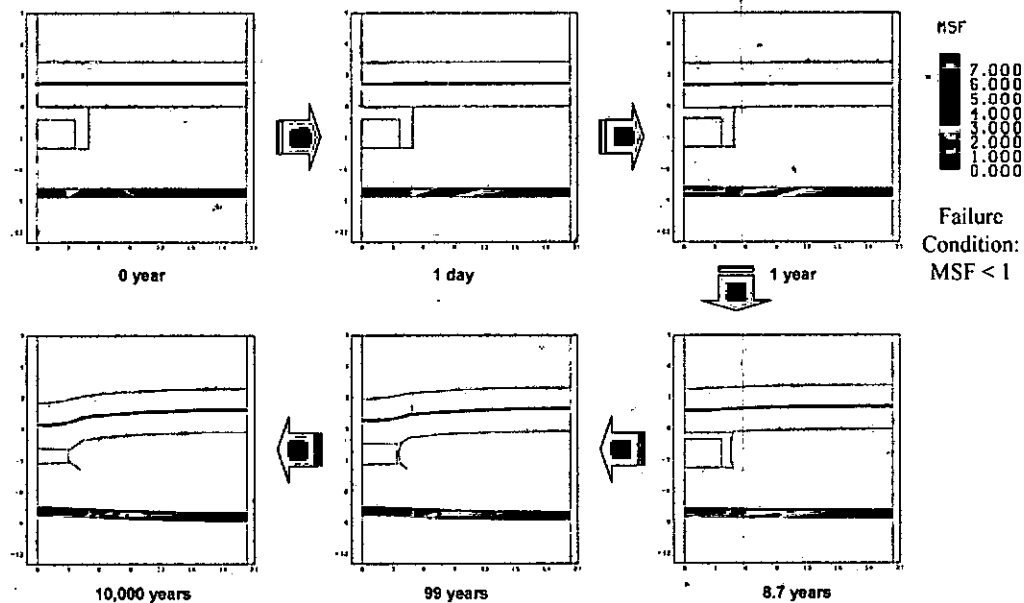


Figure 37: Changes of the shear failure zone with time in the upper and the lower anhydrite layers of the disposal room being raised 2.43 m, $f=0.0$

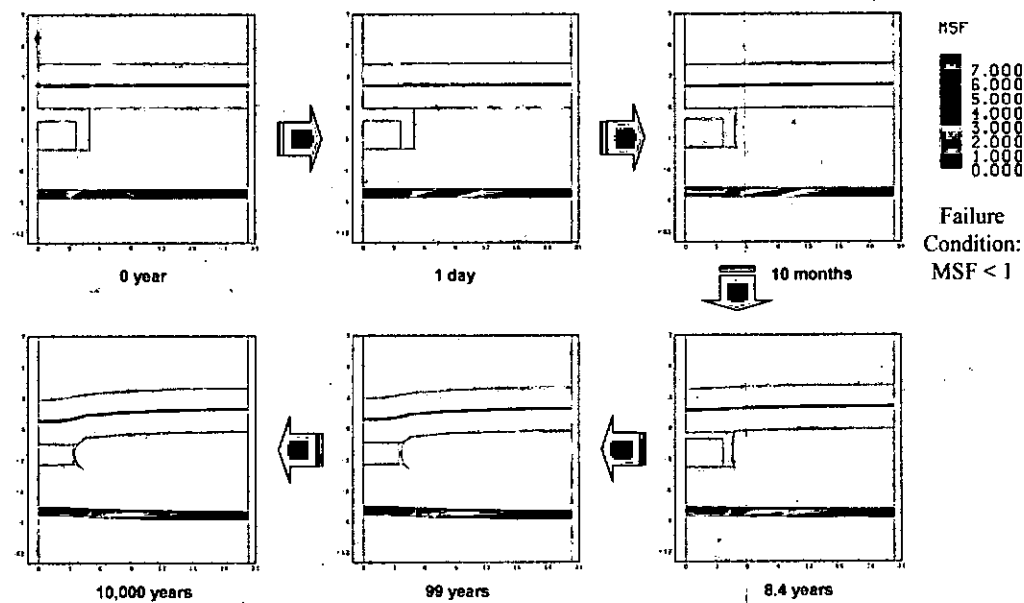


Figure 38: Changes of the shear failure zone with time in the upper and the lower anhydrite layers of the disposal room being raised 2.43 m, $f=0.4$

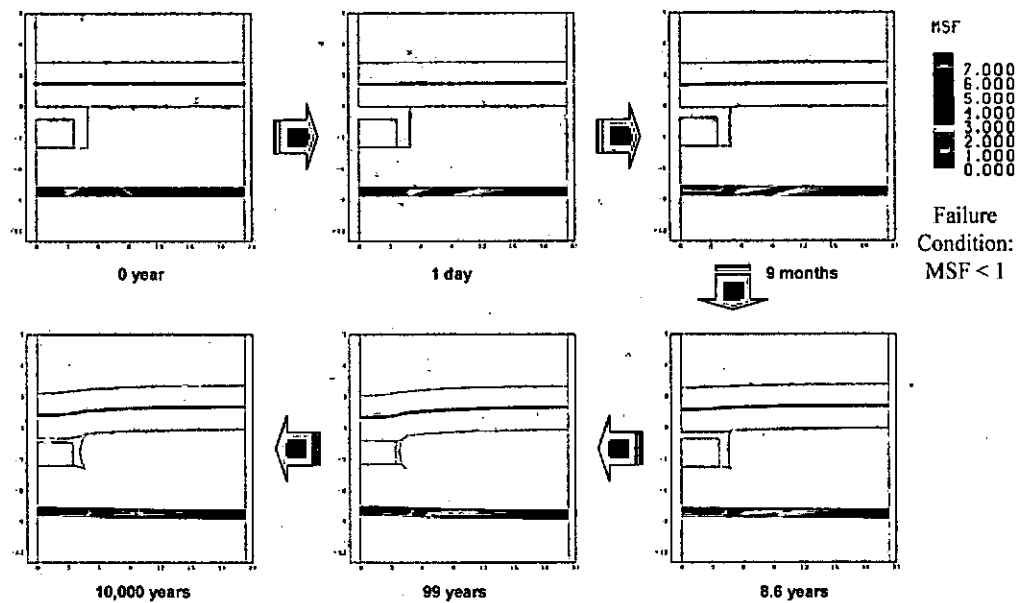


Figure 39: Changes of the shear failure zone with time in the upper and the lower anhydrite layers of the disposal room being raised 2.43 m, $f=1.0$

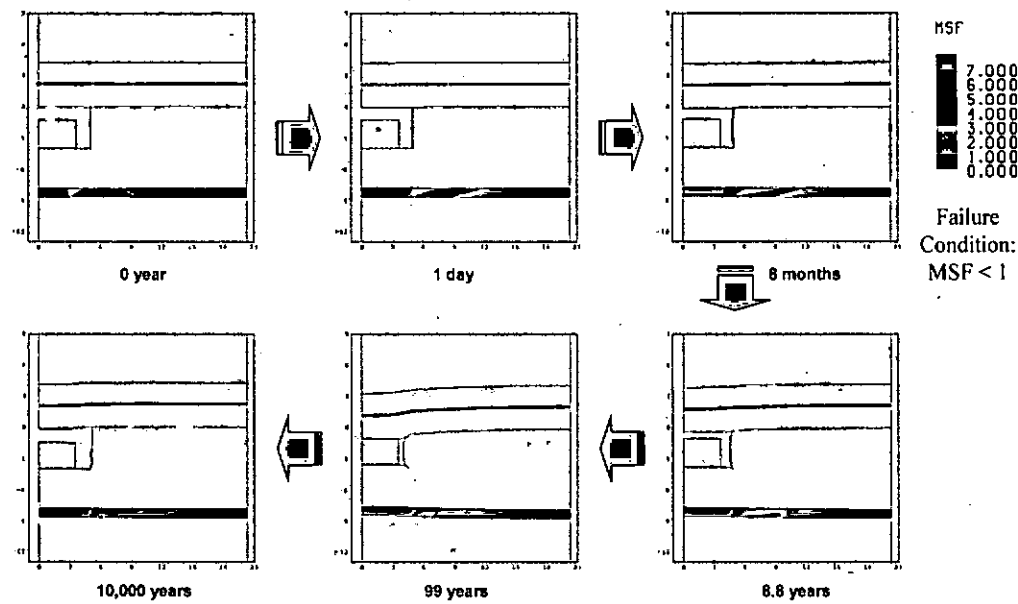


Figure 40: Changes of the shear failure zone with time in the upper and the lower anhydrite layers of the disposal room being raised 2.43 m, $f=2.0$

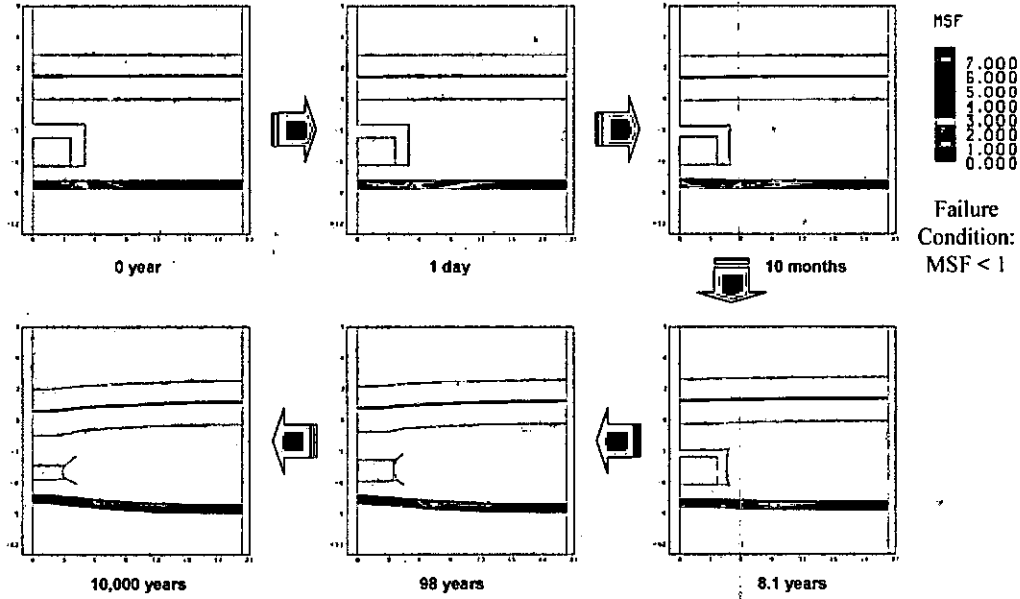


Figure 41: Changes of the shear failure zone with time in the upper and the lower anhydrite layers of the present disposal room, $f=0.0$

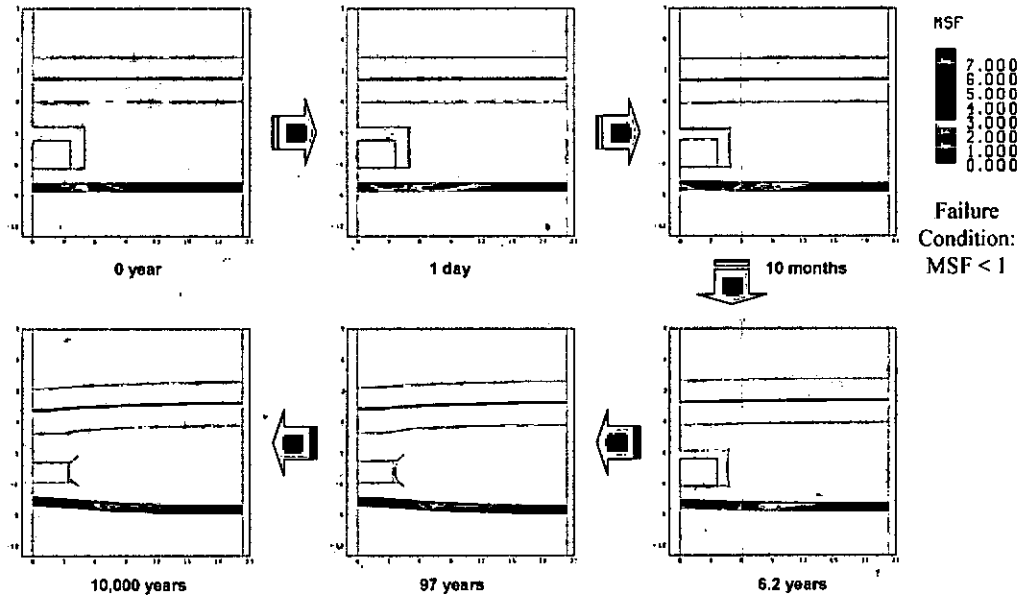


Figure 42: Changes of the shear failure zone with time in the upper and the lower anhydrite layers of the present disposal room, $f=0.4$

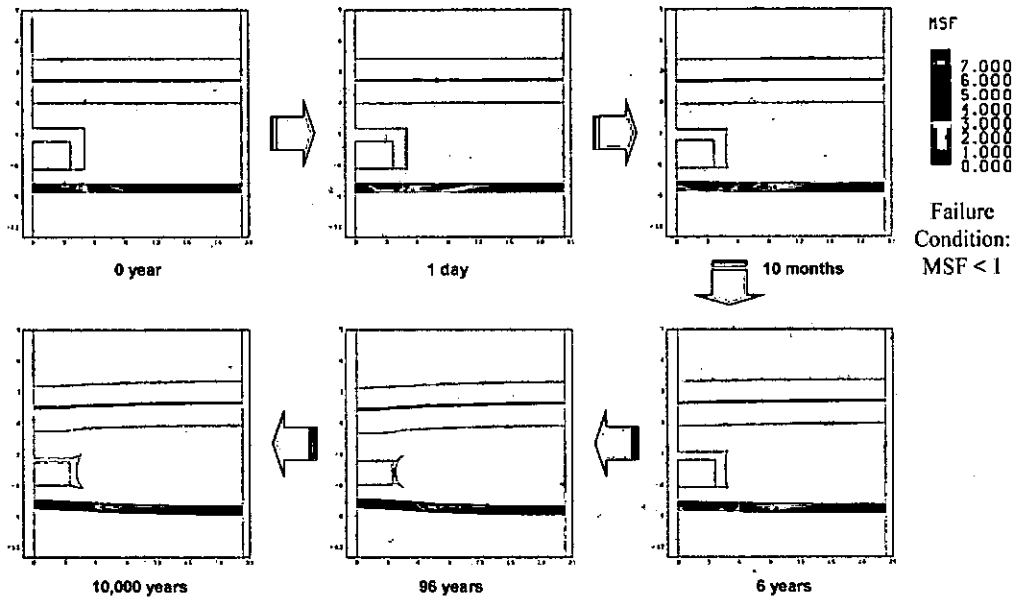


Figure 43: Changes of the shear failure zone with time in the upper and the lower anhydrite layers of the present disposal room, $f=1.0$

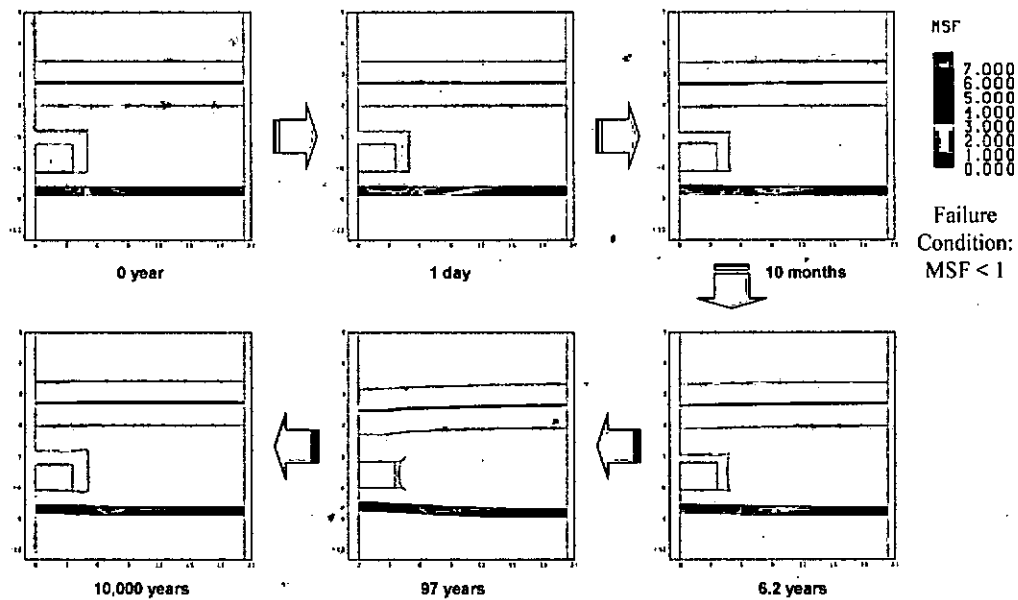


Figure 44: Changes of the shear failure zone with time in the upper and the lower anhydrite layers of the present disposal room, $f=2.0$

REVISION OF SECTION 8 SUMMARY AND CONCLUSIONS

Omitted above

Disturbed Rock Zone Calculations of the DRZ illustrate several interesting features. First the propagation of the DRZ into the surrounding rock salt does not penetrate through MB 139 in the case of both the original horizon and the raised room. The most extensive DRZ occurs at early time, say in the first ten years after the opening is mined. The DRZ above the room disappears within a short period after the ceiling of room contacts the waste.

- In the case of the raised room, the maximum extent of DRZ reaches approximately 3.8 m, the distance to the anhydrite layer (Marker Bed 139), below the room, while approximately 2.5 m over the roof of the room.
- In the case of the original horizon, the maximum thickness of upper DRZ is approximately 3.6 m over the roof of the room, while the thickness of the DRZ in the floor is 1.4 m.
- In all models the DRZ grows until the creeping salt either impinges on the waste or internal gas pressure tends to reduce the stress difference. Thereafter, the stresses trend back toward lithostatic and the DRZ criterion would suggest that the DRZ is eliminated.

Based on these modeling results, some uncertainty remains with respect to healing of the DRZ. If gas production in the room provides the counterbalancing back stress, rather than the mechanical back stress provided by the waste stack, it may be that the DRZ would not heal as it would be permeated by the gas.

Anhydrite Fracture The shear failure does not occur in either the upper or lower anhydrite layers at the moment of excavation, but appears above and below the middle of the pillar after one day the excavation. The shear stress in the anhydrite increases with time, the extent of the failure zone also increases. The internal gas pressure of the room does not affect characteristics of the shear failure zone in the anhydrite layer. The failure pattern of the present room is similar to the one of the raised room except the shear stress in the anhydrite for the present room increases faster than the raised room. The damaged anhydrite is not expected to heal as the salt in the DRZ is expected to.

Omitted below

**REVISION OF APPENDIX B: ALGEBRA FILE TO CALCULATE THE DRZ REGION
AND THE SHEAR FAILURE REGION**

```
SAVE NODAL
$
$ CONVERT STRESSES FROM PASCALS (Pa) TO MEGA-PASCALS (MPa)
$
SIGXX = SIGXX/1.0E+06
SIGYY = SIGYY/1.0E+06
SIGZZ = SIGZZ/1.0E+06
TAUXY = TAUXY/1.0E+06
VONMISES = VONMISES/1.0E+06
$
$ Compute Maximum and Minimum Principal Stresses
$
SMAX = PMAX2(SIGXX,SIGYY,TAUXY)
SMIN = PMIN2(SIGXX,SIGYY,TAUXY)
$
$ Compute mean pressure and limit it to 1.e-06
$
PRES = -( SIGXX + SIGYY + SIGZZ )/3.0
PRE = ABS(PRES) - 1.E-6
PRE2 = IFGZ(PRE,PRE,1.0E-6)
$
$ compute damage potential in the halite
$
BLOCKS 1 3
DPOT = (VONMISES/sqrt(3.0))/(3.*ABS(PRE2))
MDPOT = ENVMAX(DPOT)
$
$ compute drucker prager failure in the anhydrite
$
BLOCKS 2
PRE3 = IFEZ(PRE,1.0E-6,PRE)
SF1 = 0.45*PRE3*3. + 1.35
$
$ assume no tensile strength in the anhydrite
$
SF2 = IFGZ(SMAX,0.,SF1)
SF3 = IFLZ(SF2,0.,SF2)
$
SF = ABS(SF3)/(VONMISES/sqrt(3.0))
MSF = ENVMIN(SF)
$
$ Define time in terms of years
$
TIME = TIME/3.1536E7
$
$ Delete unneeded variables
$
DELETE PRE, PRE2, PRE3, pres,SF1,SF2,SF3
alltimes
end
```